Role of Methionine-13 in the Catalytic Mechanism of 6-Phosphogluconate Dehydrogenase from Sheep Liver†

Carlo Cervellati,‡ Franco Dallocchio,‡ Carlo M. Bergamini,‡ and Paul F. Cook*,§

Dipartimento di Biochimica e Biologia Molecolare, Università di Ferrara, via Borsari 46, 44100 Ferrara, Italy, and Department of Chemistry and Biochemistry, University of Oklahoma, 620 Parrington Oval, Norman, Oklahoma

Received November 2, 2004; Revised Manuscript Received December 2, 2004

ABSTRACT: The crystal structure of sheep liver 6-phosphogluconate dehydrogenase (6PGDH) shows marked differences in the position of the nicotinamide mononucleotide (NMN) moiety of $NADP^+$ and NADPH (Adams, J. M., Grant, H. E., Gover, S., Naylor, C. E., and Phillips, C. (1994) *Structure 2*, 651−668). A methionine side chain (Met13) interacts with the *si* face of $NADP^+$ in the complex with the oxidized coenzyme, is likely to affect the binding mode of the nicotinamide ring of $NADP^+$, and may play a role in catalysis in the 6PGDH reaction. To check this possibility we performed site-directed mutagenesis, changing M13 to a number of residues including V, I, C, F, and Q. Mutant enzymes were characterized with respect to their kinetic parameters and primary deuterium isotope effects. All mutations resulted in a decrease in affinity of the enzyme for $NADP^+$, but not NADPH. In addition, the M13 to C (M13C), M13F, and M13Q mutant enzymes exhibited a decrease of at least an order of magnitude in V/E_t. The deuterium isotope effects on V and V/K_{6PG} were decreased to about 1.2 for the M13F and M13C mutant enzymes, while they were increased to about 2.4 for the M13Q enzyme (a value of 1.8−1.9 is obtained for the wild-type enzyme). In at least three instances changes in the overall rate of the oxidative decarboxylation reaction relative to other steps along the reaction pathway were observed. Isotope effects indicate that the hydride transfer steps can become either more or less rate-determining dependent on the substitution. Data are consistent with a significant role of M13 in the orientation of the cofactor nicotinamide ring in the mechanism of 6PGDH, likely with respect to geometry and distance of the ring from C3 of 6PG.

6-Phosphogluconate dehydrogenase (6PGDH; EC 1.1.1.44)[1] catalyzes a reversible oxidative decarboxylation of 6-phosphogluconate to ribulose 5-phosphate and CO_2, with $NADP^+$ as the oxidant. Available information suggests that oxidative decarboxylation of 6PG to the 1,2-enediol of ribulose 5-phosphate proceeds via a stepwise mechanism, with hydride transfer preceding decarboxylation (*1*, *2*). In the last step of the catalytic cycle the enediol is tautomerized to ribulose 5-phosphate. The pH dependence of kinetic parameters (*3*, *4*) in conjunction with structural data (*5*) and site-directed mutagenesis (*6*, *7*) has suggested that catalysis proceeds via a general base−general acid mechanism involving K183 and E190 acting as base and acid, respectively (Figure 1). In this mechanism K183 accepts the proton from the 3-hydroxyl of 6PG as a hydride is transferred from C-3 of 6PG to $NADP^+$. The resulting 3-keto-6-phosphogluconate intermediate is then decarboxylated to give the enediol of Ru5P, with K183 now acting as a general acid to donate a proton to the C-3 carbonyl group of the keto intermediate. Finally, E190 assists in the tautomerization of the enediol to the final ketone product, with K183 now accepting a proton from the 2-hydroxyl of the enediol intermediate (*7*).

As displayed in Figure 2, the bound conformations of an NADP analogue, NBr^8ADP, and of NADPH differ markedly with respect to the nicotinamide ring of the cofactor, while much smaller changes overall are observed for the AMP portion of the cofactors. In the E:NADPH complex, the nicotinamide ring is anti, while in the E:NADP complex it is closer to the syn conformation. The syn conformation of the E:NADP complex appears to be stabilized by a pyrophosphate ion present in the crystallization solution. The orientation shown in the complex is very similar to that seen for NAD^+ in glyceraldehyde 3-phosphate dehydrogenase, and may represent the most energetically stable form in these enzymes. The nicotinamide ring of $NADP^+$ may be further stabilized by interaction with the polarizable sulfur of the conserved M13, Table 1. Of the 27 entries given in the list, from higher animals and plants to bacteria, all have M13 conserved. On the basis of a comparison of the interactions between protein and cofactor, NADPH makes more hydrogen-bonding contacts than does $NADP^+$. The difference between

† This work was supported by a grant from the National Science Foundation to P.F.C. (MCB 009127), and grants to B.G.H. from the National Institutes of Health (AI24155; AI41552) and the Robert A. Welch Foundation (BK1309), and the Grayce B. Kerr endowment to the University of Oklahoma for the research of P.F.C.

* Corresponding author. Tel: 405-325-4581. Fax: 405-325-7182. E-mail: pcook@chemdept.chem.ou.edu.

‡ Università degli Studi di Ferrara.

§ University of Oklahoma.

[1] Abbreviations: Hepes, 4-(2-hydroxyethyl)-1-piperazineethanesulfonic acid; 6PG, 6-phosphogluconate; 6PGDH, 6-phosphogluconate dehydrogenase; Ru5P, ribulose 5-phosphate; NMN, nicotinamide mononucleotide; 3-d-6PG, 3-*deuterio*-6-phosphogluconate; 2-deoxy-6PG, 2-deoxy-6-phosphogluconate; 2′5′ADP agarose, 2′,5′-adenosine diphosphate agarose; TEA, triethanolamine.

10.1021/bi0476679 CCC: $30.25
Published on Web 01/25/2005

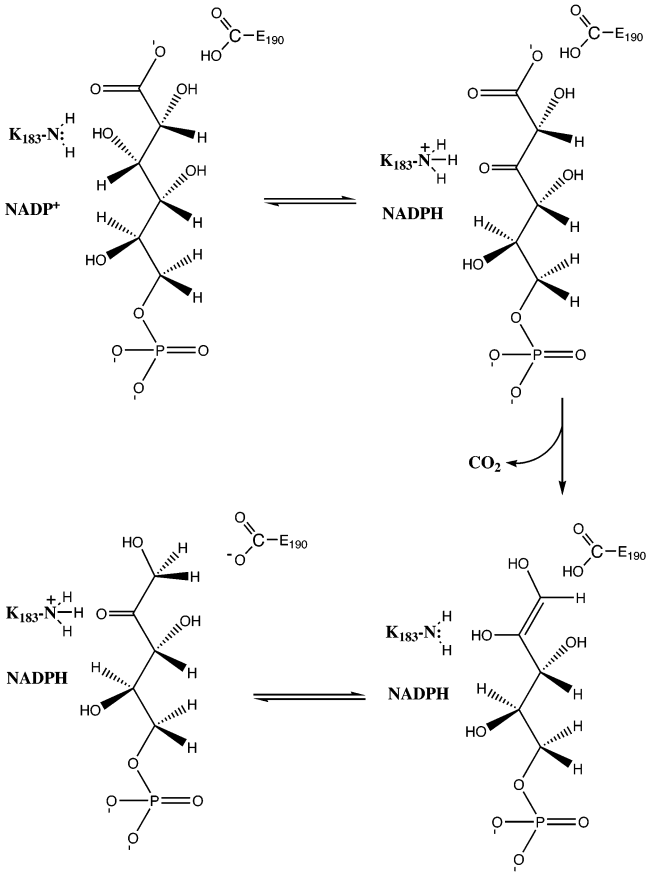

FIGURE 1: Proposed mechanism for 6-phosphogluconate dehydrogenase.

the two is essentially due to the difference in conformation of the nicotinamide ring. The change in the position of the nicotinamide ring of NADPH brings its functional groups within hydrogen-bonding distance to amino acid side chains in the coenzyme- and substrate-binding domains. On the other hand, the nicotinamide ring of $NADP^+$ is within hydrogen-bonding distance to only 2 amino acids in the coenzyme-binding domain. Specifically, the oxygen and nitrogen of the carboxamide side chain of $NADP^+$ are within hydrogen-bonding distance to the main chain NH of M13 and the carboxylate of E131, respectively.

The location of the nicotinamide ring of $NADP^+$ and NADPH could represent the position of the coenzyme prior to and after the hydride transfer step (*7*), i.e., the coenzyme may isomerize during the time course of the reaction. Similar hypotheses have been formulated in two recently studied NAD-dependent aldehyde dehydrogenases (*8*, *9*). The authors postulate that achieving the correct position of the nicotinamide ring of the coenzyme in oxidized and reduced states is crucial to the occurrence of two different catalytic steps, oxidation of the thiohemiacetal and hydrolysis of the resulting ester. In the case of 6PGDH, Rippa (*10*−*14*) suggested, prior to the availability of the 3-D structure of 6PGDH, a catalytic but nonredox role for NADPH. It was demonstrated that NADPH was involved in facilitating decarboxylation of the 3-keto intermediate utilizing 2-deoxy-6-phosphogluconate as an analogue of 6PG and in activating the onset of tautomerization of the enediol to Ru5P.

In this paper we investigate the effect of substitution of the methionine at position 13 on the mechanism of 6PGDH, focusing on the catalytic relevance of positioning the nicotinamide ring of the cofactor. Site-specific mutagenesis has been used to change M13 to 5 other amino acids, V, I, C, F, and Q. Data are consistent with a role of M13 in orienting the nicotinamide ring of the cofactor with respect to geometry and distance, thereby optimizing the geometry for the hydride transfer step, and perhaps the decarboxylation step in the 6PGDH reaction.

MATERIALS AND METHODS

Chemicals and Reagents. Mutagenesis and sequencing primers were from either Biosynthesis or Gibco-BRL. The QuickChange site-directed mutagenesis kit was from Stratagene. The DNA cycle sequencing system was purchased from Promega, while the QIAprep Spin Miniprep and the QIAexpress kits were from QIAGEN. Restriction endonucleases and isopropyl-β-D-thiogalactopyranoside were purchased from Gibco-BRL.

Ampicillin, kanamycin, 6-phosphogluconate, $NADP^+$, TEA, Hepes, hexokinase, acetylphosphate, acetate kinase, glucose 6-phosphate, and glucose 6-phosphate dehydrogenase were from Sigma, while 3-deuterio-glucose was purchased from Omicron Biochemicals, Inc. All other chemicals and reagents were obtained from commercial sources and were of the highest possible purity available.

Bacterial Strain and Plasmids. The *Escherichia coli* strain XL1-Blue was the host strain for plasmids containing M13 mutations, and M15(pREP4) was used as a host for expression. The plasmid pQE30 was used as both mutagenesis and expression vectors.

Site-Directed Mutagenesis. Site-directed mutagenesis was performed on double-stranded DNA prepared from recombinant plasmid pPGDH.LC4 (15) using QuickChange site-directed mutagenesis and the syntethic oligonucleotide primers listed in Table 2. Mutations were confirmed by sequence analysis using the above-mentioned sequencing kit. Resulting plasmids were designated as pEM13V, pEM13I, pEM13C, pEM13F, and pEM13Q.[2] Newly prepared DNA was then recovered from the recipient strain XL1-Blue and subsequently transformed into M15(PREP4) using an EC100 electroporator according to the manufacturer's specifications. Frozen stocks of strains harboring plasmid were stored in LB/ampicillin/kanamycin medium containing 15% glycerol at −80 °C.

Growth and Purification Conditions. The bacterial strains containing each mutant were grown in 10 L of LB/ampicillin/kanamycin medium until an absorbance of 0.7 at 600 nm was reached, at which time isopropyl-β-D-thiogalactopyranoside was added to a final concentration of 1 mM and growth was continued for an additional 4 h. Bacterial cells were harvested by centrifugation at 7000*g* for 10 min, resuspended in 3 vol of TEA buffer (50 mM TEA (titrated with HCl), pH 8.0, 5 mM β-mercaptoethanol), and stored at −20 °C. Wild-type and mutant 6PGDHs were purified by a slight modification of a previous procedure (*15*). The thawed bacterial cell paste in TEA buffer was sonicated with a

[2] The notation used throughout for mutant enzymes makes use of the one letter abbreviation for the amino acid, followed by the position, which is followed by the one letter abbreviation for the amino acid substitution. Thus for replacement of methionine at position 13 with cysteine, the abbreviation M13C is used.

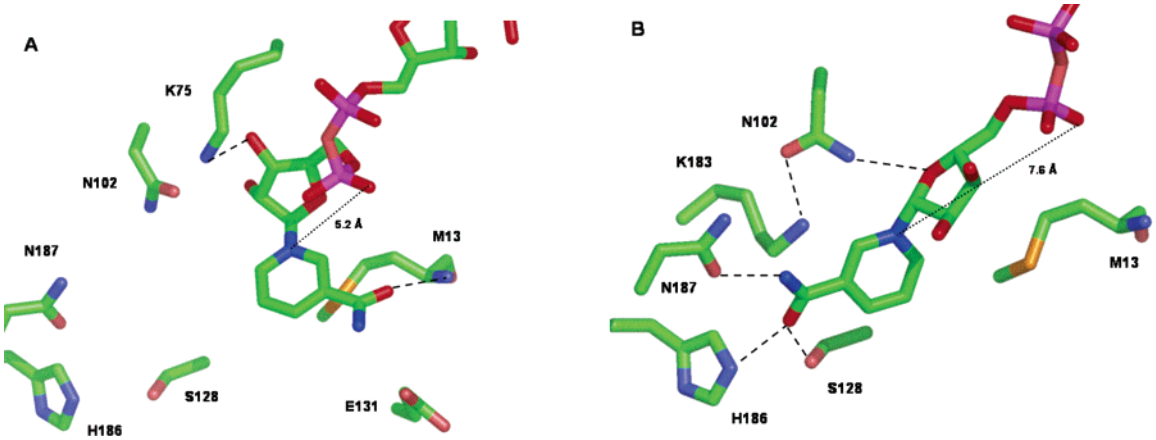

FIGURE 2: Close-up view of the dinucleotide binding site in the binary E:N(8-Br-ADP) (left) and E:NADPH (right) complexes. In the figures green is C, blue is N, red is O, magenta is P, and orange is S. Figures were created using PyMOL from DeLano Scientific LLC (www.pymol.org). Accession numbers in the PDB are 1PGN and 1PGO for the E:N(8-Br-ADP) and E:NADPH structures, respectively.

Table 1: Multiple Sequence Alignment of 6PGDH around Methionine 13 (Bold)

species	sequence around M13																					ref
Homo sapiens	A	D	I	A	L	I	G	L	A	V	**M**	G	Q	N	L	I	L	N	M	N	D	21
Ovis aries	A	D	I	A	L	I	G	L	A	V	**M**	G	Q	N	L	A	L	N	I	E	R	22
Zea mays	T	R	I	G	L	A	G	L	A	V	**M**	G	Q	N	L	A	L	N	I	A	E	23
Cunninghamella elegans	A	D	I	G	L	I	G	L	A	V	**M**	G	Q	N	L	I	L	N	M	N	D	24
Pirellula sp.	C	D	F	G	L	I	G	L	A	V	**M**	G	E	N	L	A	L	N	V	E	S	25
Drosophila melanogaster	A	D	I	A	L	I	G	L	A	V	**M**	G	Q	N	L	I	L	N	M	D	E	26
Drosophila simulans	A	D	I	A	L	I	G	L	A	V	**M**	G	Q	N	L	I	L	N	M	D	E	27
Trypanosoma brucei	M	D	V	G	V	V	G	L	G	V	**M**	G	A	N	L	A	L	N	I	A	E	28
Thermoanaerobacter tencongensis	N	D	V	G	L	I	G	L	A	V	**M**	G	Q	N	F	A	L	N	M	A	R	29
Saccharomyces cerevisiae	G	D	L	G	L	V	G	L	A	V	**M**	G	Q	N	L	I	L	N	A	A	D	30
Buchnera aphidicola	Q	Q	I	G	V	V	G	M	A	V	**M**	G	R	N	L	A	L	N	I	E	S	31
Escherichia coli	Q	Q	I	G	V	V	G	M	A	V	**M**	G	R	N	L	A	L	N	I	E	S	32
Shigella flexneri	Q	Q	I	G	V	V	G	M	A	V	**M**	G	A	N	L	A	L	N	I	E	S	33
Salmonella typhimurium	Q	Q	I	G	V	V	G	M	A	V	**M**	G	R	N	L	A	L	N	I	E	S	34
Klebsiella pneumoniae	Q	Q	I	G	V	V	G	M	A	V	**M**	G	A	N	L	A	L	N	I	E	S	35
Lactobacillus lactis	A	N	F	G	V	V	G	M	A	V	**M**	G	K	N	L	A	L	N	V	E	S	36
Actinobacter actinomycetemcomitans	G	D	I	G	V	I	G	L	A	V	**M**	G	Q	N	L	I	L	N	M	N	D	37
Synecocistis sp.	R	T	F	G	V	I	G	L	A	V	**M**	G	E	N	L	A	L	N	V	E	S	38
Synechococcus sp.	Q	Q	F	G	L	I	G	L	A	V	**M**	G	E	N	L	A	L	N	I	E	R	39
Haemophilus influenzae	G	D	I	G	V	I	G	L	A	V	**M**	G	Q	N	L	I	L	N	M	N	D	40
Ceratitis capitata	A	D	I	A	L	I	G	L	A	V	**M**	G	Q	N	L	V	L	N	M	N	D	41
Treponema pallidum	A	D	I	G	F	I	G	L	A	V	**M**	G	E	N	L	V	L	N	I	E	R	42
Bacillus licheniformis	N	T	I	G	V	I	G	L	G	V	**M**	G	S	N	I	A	L	N	M	A	S	43
Bacillus subtilis	N	S	I	G	V	I	G	L	G	V	**M**	G	S	N	I	A	L	N	M	A	N	44
Mycobacterium leprae	A	Q	I	G	W	T	G	L	A	V	**M**	G	S	N	I	A	R	N	F	A	R	45
Chlamydia trachomatis	T	D	I	G	L	I	G	L	A	V	**M**	G	Q	N	L	V	L	N	M	V	D	46

Table 2: Sequence of Oligonucleotide Primers[a]

$M13C_f$	GGACTGGCTGTC**TGC**GGCCAGAACTTA
$M13C_r$	CCTGACCGACAG**ACG**CCGGTCTTGAAT
$M13V_f$	GGACTGGCTGTC**GTT**GGCCAGAACTTA
$M13V_r$	CCTGACCGACAG**CAA**CCGGTCTTGAAT
$M13Q_f$	GGACTGGCTGTC**GAG**GGCCAGAACTTA
$M13Q_r$	CCTGACCGACAG**CTC**CCGGTCTTGAAT
$M13I_f$	GGACTGGCTGTC**ATT**GGCCAGAACTTA
$M13I_r$	CCTGACCGACAG**TAT**CCGGTCTTGAAT
$M13F_f$	GGACTGGCTGTC**TTC**GGCCAGAACTTA
$M13F_r$	CCTGACCGACAG**AAG**CCGGTCTTGAAT

[a] Subscripts f and r represent forward and reverse primers. Mutated codons are in bold.

Misonix Inc. model XL ultrasonic liquid processor in 200 mL batches on ice for a total time of 2 min, with on/off intervals of 30 s. The sonicated suspension was centrifuged at 12000*g* for 40 min to remove cell debris. The His-tagged proteins, recovered in the soluble fraction, were purified using chromatographic adsorbents supplied by Qiagen. The cellular extract was mixed batchwise with Ni-NTA resin and, after stirring for 1 h, was poured into a column. The column was washed with 4−5 vol of TEA buffer, and subsequently the protein was eluted with the same buffer plus 150 mM imidazole. The eluted protein was pooled and loaded onto a column with 10 mL of 2′5′ADP agarose. The resin was extensively washed with TEA buffer to eliminate any residual contamination with imidazole, which was found to affect the activity of 6PGDH. The protein was eluted with 150 mM sodium pyrophosphate, pH 7.5. The mutant and wild-type proteins were purified in an identical manner, and all enzymes were stored at 4 °C in the same buffer used for the elution from 2′5′ADP agarose.

The specific activity of wild-type enzyme obtained from the above purification procedure was 3-fold higher when compared with that obtained by the original method, i.e., without the 2′5′ADP agarose chromatography. This marked improvement was possibly due to the ability of 2′5′ADP

agarose to separate the active form of the enzyme from any inactive protein. As described by Silverberg and Dalziel (*16*) only the active native enzyme binds coenzymes. Enzyme concentration was determined by means of the Bio-Rad protein assay kit using BSA as a standard.

Synthesis of 3-d-6PG. The 3-*d*-glucose was enzymatically converted to 3-*d*-glucose 6-phosphate as described (*2*). The extent of conversion to the product of the reaction was determined using enzymatic end-point assay with glucose-6-phosphate dehydrogenase. Upon completion of the reaction the solution was adjusted to pH 4.5 to denature the enzymes present in the mixture. Enzymes were removed by Amicon ultrafiltration through a PM-30 semipermeable membrane filter, and the resulting solution was treated with Dowex 50W-H^+ and with acid-washed and heat-activated charcoal and stirred for 1 h to remove Mg^{2+} and nucleotides. The filtered solution, containing the resultant glucose 6-phosphate, was then bromine oxidized as described below.

The solution pH was adjusted to 5.4 with acetic acid, and a 3-fold molar excess of 1% bromine solution was added, maintaining the pH of the reaction around 5−5.8 with 1 M NaOH. Addition was stopped when no further change of pH was detected. The oxidized product was purified using 6 mL of Dowex AG1 anion-exchange resin (previously charged with HCl) by a 200 mL linear gradient to 0.6 M NaCl, in the same solvent. The eluted pool was then lyophilized. To eliminate remaining salts the lyophilized powder was dissolved in water, and the 3-d-6PG was precipitated with barium acetate/ethanol. The suspensions were vigorously mixed until the two phases disappeared, stored on ice for 15 min, and then centrifuged at 3000*g*. Pellets were resuspended in 1 mL of water and 4 mL of ethanol and centrifuged at 3000*g*. Then, 5 mL of ether was added to each tube, and the precipitate was harvested by centrifugation at 3000*g*. The contents of each tube were dried, followed by addition of 1 mL of water to each tube, and the contents of all tubes were then pooled and Dowex 50W-H^+ was added to remove residual barium. The resin was then removed, leaving the 3-d-6PG. As a probe of chemical purity, the isotope effect for wild-type enzyme was measured. The value obtained was identical, within error, to that reported in the literature confirming the effectiveness of the preparation.

Initial Velocity Studies. Initial velocity studies were performed using a Kontron Uvikon 930 spectrophotometer measuring the change in absorbance at 340 nm due to NADPH formation ($\epsilon_{340} = 6220\ M^{-1}\ cm^{-1}$). Reactions were carried out in a 1 mL volume using 1 cm path length cuvettes. The kinetic parameters were obtained by measuring the initial velocity in 100 mM Hepes (titrated with KOH), pH 7 either varying 6PG at a saturating level of $NADP^+$ (0.6 mM) or varying $NADP^+$ at a saturating level of 6PG (1 mM). The enzyme was diluted 5-fold before each measurement, in order to diminish the concentration of pyrophosphate derived from the elution of 2′5′ADP sepharose in the reaction mixture.

The K_i for NADPH as an inhibitor competitive vs $NADP^+$ was measured with 6PG equal to its K_m (E:NADP) and at saturating **(**$20K_m$**)** concentration (E:6PG:NADPH). Data were obtained for the wild-type and mutant enzymes as above at pH 7.

Primary Deuterium Isotope Effects. Substrate concentrations were determined by enzymatic end point in triplicate using 6PGDH. Primary isotope effects with 3-d-6PG were obtained by direct comparison of initial velocities determined by monitoring fluorescence emission at 460 nm due to the formation of NADPH in the time course of the reaction using a Perkin-Elmer LS 55 fluorimeter. The use of fluorescence as a probe, unlike the use of absorbance described above, permits concentrations of $NADP^+$ lower than 1 μM to be used, taking advantage of high sensitivity of the instrument. ^DV and $^D(V/K_{NADP})$ were measured by varying NADP at saturating levels of either 6PG or 3-d-6PG.

Data Processing. Reciprocal initial velocities were plotted against reciprocal substrate concentrations. Data were fitted to the appropriate rate equation using Basic versions of the computer programs developed by Cleland (*17*). Initial velocity data were fitted using eq 1,

$$v = \frac{V\mathbf{A}}{K_a + \mathbf{A}} \tag{1}$$

where v and V are initial and maximum velocities, respectively, **A** is the reactant concentration (either 6PG or NADP), and K_a is the Michaelis constant for either 6PG or NADP.

Deuterium kinetic isotope effect data were fitted using eq 2 allowing for independent isotope effects on V and V/K.

$$v = \frac{V\mathbf{A}}{K_a(1 + F_iE_{V/K}) + \mathbf{A}(1 + F_iE_V)} \tag{2}$$

In eq 2 F_i is the fraction of deuterium label in the substrate (determined on the basis of 98 atom % D in the 3-*d*-glucose), while $E_{V/K}$ and E_V are the isotope effects minus 1 on V/K and V, respectively. All other terms are as defined above.

RESULTS

Spectral Properties and Overall Structure of Mutant Enzymes. The spectral properties of recombinant wild-type and mutant 6PGDHs were explored as an initial check for general perturbations of the protein structure brought about by mutation at Met13. Far UV CD spectra were recorded (data not shown) for all mutant enzymes, and all were identical to the spectrum of the wild-type enzyme once adjusted for protein concentration. Thus the mutations introduced in the enzyme's active site do not perturb the secondary structure of the M13 mutant enzymes, and any changes are likely localized to the active site. In addition, tryptophan fluorescence emission spectra, obtained upon excitation at 290 nm (data not shown), were identical for all mutant enzymes to that of the wild-type enzyme, indicating conservation of the microenvironment of tryptophan residues of the protein.

Kinetic Parameters of the Mutant Proteins. Initial velocity studies were carried out at pH 7 by measuring the initial rate as a function of $NADP^+$ concentration at a fixed, saturating concentration of 6PG, and conversely as a function of 6PG concentration at saturating concentrations of $NADP^+$. Data are summarized in Table 3.

No significant change was observed in K_{6PG} (20−30 μM) of the M13 mutant enzymes with respect to the value of the wild-type enzyme (data not shown). In contrast, K_{NADP} increased by at least an order of magnitude compared to the wild-type enzyme for all but M13C mutation, which showed a 3-fold increase. The difference in behavior of the M13C mutant enzyme may result from the conservation of the sulfur

Table 3: Summary of Kinetic Parameters for the M13 Mutants of 6PGDH

enzyme	K_{NADP}[a] (μM)	V/E_t (s^{-1})	^{D}V	$V/K_{NADP}E_t$ (M^{-1} s^{-1})	$^{D}(V/K_{NADP})$
wild type	2 ± 1	9.3 ± 0.1	1.8 ± 0.1	$(4.6 \pm 0.6) \times 10^6$	1.9 ± 0.3
M13I	32 ± 3 (16)[b]	9.5 ± 0.1	2.4 ± 0.6	$(2.9 \pm 0.9) \times 10^5$ (15)[c]	2.4 ± 0.8
M13V	26 ± 9 (13)	9.51 ± 0.08	1.7 ± 0.4	$(3.7 \pm 0.4) \times 10^5$ (12)	1.9 ± 0.4
M13F	19 ± 6 (9.5)	0.51 ± 0.03 (18.6)[c]	1.3 ± 0.2	$(2.6 \pm 0.7) \times 10^4$ (176)	1.2 ± 0.2
M13C	6.4 ± 0.8 (3.2)	1.14 ± 0.04 (8.1)	1.3 ± 0.3	$(1.8 \pm 0.6) \times 10^5$ (25)	1.3 ± 0.4
M13Q	19 ± 1 (9.5)	1.14 ± 0.05 (8.1)	2.8 ± 0.3	$(5.9 \pm 0.1) \times 10^4$ (78)	3.1 ± 0.1

[a] Values are ± S.E. [b] Fold increase. [c] Fold decrease.

Table 4: Summary of K_i for NADPH for M13 Mutants of 6PGDH[a]

enzyme	$K_{i\ NADPH}$ (μM)[b]	$K_{i\ NADPH}$ (μM)[c]	$K_{NADP}/K_{i\ NADPH}$[c] (μM)
wild type	0.8 ± 0.5	1.1 ± 0.4	1.8
M13I	0.8 ± 0.5	1.0 ± 0.2	1.6
M13V	1.3 ± 0.5	6 ± 2	4.3
M13F	0.9 ± 0.7	1.5 ± 0.6	12.7
M13C	5.0 ± 1.0	0.65 ± 0.15	9.8
M13Q	1.3 ± 0.3	2.1 ± 0.6	9.5

[a] Values are ± standard deviation. [b] Obtained with 6PG = K_{6PG}. Corrected to zero concentration of 6PG. [c] Obtained with 6PG = $20K_{6PG}$.

atom, since, as suggested by Adams (*5*), the sulfur could contribute to $NADP^+$ binding. The value of V/E_t is decreased by about an order of magnitude compared to the wild-type enzyme for the M13F, M13C, and M13Q mutant enzymes, while no change was observed for the M13V and M13I mutations. Since $V/K_{NADP}E_t$ is the ratio of V/E_t and K_{NADP}, the decrease in the second-order rate constant reflects the change in V/E_t for M13I and M13V, while it is greater for the other three mutant enzymes.

Kinetic Deuterium Isotope Effects. The kinetic deuterium isotope effects on V and V/K_{NADP} were measured to determine whether substitution for M13 results in a change in the rate of the hydride transfer step relative to others along the reaction pathway. As shown in Table 3, equal isotope effects on the two parameters are obtained in the case of the wild-type enzyme consistent with the rapid equilibrium random kinetic mechanism of 6PGDH (*4*). The equality of the isotope effects on the two parameters holds for all of the mutant enzymes. While the deuterium isotope effects on the M13V and M13I mutant enzymes are identical within error to those of the wild-type enzyme, those measured with the other mutant enzymes are significantly different. In particular, the isotope effects are lower and close to unity for M13F and M13C mutant enzymes, while those for the M13Q mutant enzyme are higher.

Inhibition and Dissociation Constants for NADPH. The inhibition constants for NADPH vs $NADP^+$, obtained at saturating 6PG for the mutant enzymes, are given in Table 4. In addition, the K_i for NADPH as a competitive inhibitor vs $NADP^+$ at K_m levels of 6PG was measured to target free enzyme. Data are summarized in Table 4.

DISCUSSION

The main aim of our work was to determine whether methionine 13 helps to orient the nicotinamide ring of $NADP^+$ bound to 6PGDH for optimum hydride transfer from C3 of 6PG, and thus plays a role in the enzyme's overall reaction. The putative role of M13 was postulated on the basis of differences in its interaction with the nicotinamide ring of oxidized and reduced cofactors in the binary complex and a multiple sequence alignment of 6PGDHs from a variety of species from bacteria to man, Table 1, which showed complete conservation of the methionine near the N-terminus. As a result site-directed mutagenesis was used to change M13 to other hydrophobic or polar uncharged amino acids and to determine the effect of the substitutions on the 6PGDH reaction using steady-state kinetic and isotope effects. Below we discuss the results in the context of the structural and mechanistic information available for 6PGDH.

Kinetic Model. Oxidative decarboxylation of 6PG catalyzed by 6PGDH proceeds by a stepwise mechanism, with dehydrogenation preceding decarboxylation as suggested by multiple $^2H/^{13}C$ isotope effects (*2*). Multiple solvent deuterium/$^2H/^{13}C$ isotope effects suggest the presence of a kinetically significant isomerization of the E:NADP:6PG complex prior to catalysis (*18*). Finally, the equality of the primary deuterium isotope effects on V, V/K_{6PG}, and V/K_{NADP} are indicative of a rapid equilibrium random kinetic mechanism (*4*, *19*). On the basis of the above assumptions, and under conditions where 6PG is maintained saturating, the following kinetic scheme can be written for 6PGDH:

$$\mathrm{EA} \underset{k_4}{\overset{k_3\mathrm{B}}{\rightleftharpoons}} \mathrm{EAB} \underset{k_6}{\overset{k_5}{\rightleftharpoons}} \mathrm{E'AB} \underset{k_8}{\overset{k_7}{\rightleftharpoons}} \mathrm{E'XR} \xrightarrow{k_9} \mathrm{E'QR} \xrightarrow{k_{11}} \mathrm{E'R} \xrightarrow{k_{13}} \mathrm{E} \tag{3}$$

where A, B, X, Q, and R represent 6PG, $NADP^+$, 3-keto-6PG, ribulose 5-phosphate, and NADPH, E′ represents the isomerized form of the enzyme, k_3 and k_4 are binding and dissociation rate constants for $NADP^+$, k_5 and k_6 are rate constants for the isomerization, k_7 and k_8 are for forward and reverse hydride transfer, k_9 represents decarboxylation and release of CO_2, k_{11} represents tautomerization and release of ribulose 5-phosphate, and k_{13} represents release of NADPH.

Given the rapid equilibrium nature of the mechanism, central complex interconversion is rate-limiting (steps included from EAB to E′QR, and thus $k_4 > k_5$, while k_{11}, $k_{13} > k_7$. Using these assumptions, expressions for V and V/K_{NADP} are given in eqs 4 and 5,

$$V = \frac{\dfrac{k_7}{1+\dfrac{k_6}{k_5}}}{1+\dfrac{k_7\left(\dfrac{1}{k_5}+\dfrac{1}{k_9}\right)}{1+\dfrac{k_6}{k_5}}+\dfrac{k_8}{k_9}} \tag{4}$$

$$\frac{V}{K_{NADP}} = \frac{\dfrac{k_3k_5k_7}{k_4k_6}}{1+\dfrac{k_7}{k_6}+\dfrac{k_8}{k_9}} \tag{5}$$

and K_{NADP} is the ratio of V and V/K_{NADP},

$$K_{NADP} = K_d\left[\frac{k_6k_7\left(1+\frac{k_7}{k_6}+\frac{k_8}{k_9}\right)}{k_5k_7\left(1+\frac{k_6}{k_5}\right)\left(1+\frac{k_7\left(\frac{1}{k_5}+\frac{1}{k_9}\right)}{1+\frac{k_6}{k_5}}+\frac{k_8}{k_9}\right)}\right] \quad (6)$$

Using the same assumptions as those discussed above, expressions for the isotope effects on V and V/K_{NADP} are given below:

$$^{D}V = \frac{^{D}k_7+\frac{k_7\left(\frac{1}{k_5}+\frac{1}{k_9}\right)}{1+\frac{k_6}{k_5}}+(^{D}K_{eq})\left(\frac{k_8}{k_9}\right)}{1+\frac{k_7\left(\frac{1}{k_5}+\frac{1}{k_9}\right)}{1+\frac{k_6}{k_5}}+\frac{k_8}{k_9}} \quad (7)$$

$$^{D}\left(\frac{V}{K_{NADP}}\right) = \frac{^{D}k_7+\frac{k_7}{k_6}+(^{D}K_{eq})\left(\frac{k_8}{k_9}\right)}{1+\frac{k_7}{k_6}+\frac{k_8}{k_9}} \quad (8)$$

where $^{D}k_7$ is the intrinsic deuterium isotope effect on the hydride transfer step, and $^{D}K_{eq}$ is the equilibrium isotope effect on hydride transfer (1.18 for oxidation of a secondary alcohol (*20*). Since the kinetic isotope effects on V and V/K are equal to one another for the wild-type and each of the mutant enzymes, either $k_6 = (1 + k_6/k_5)/(1/k_5 + 1/k_9)$ or more likely k_6, $(1 + k_6/k_5)/(1/k_5 + 1/k_9) > k_7$. If the latter is correct, eqs 4−8 reduce to

$$V = \frac{k_7}{\left(1+\frac{k_6}{k_5}\right)\left(1+\frac{k_8}{k_9}\right)} \quad (9)$$

$$\frac{V}{K_{NADP}} = \frac{k_3k_5k_7}{k_4k_6\left(1+\frac{k_8}{k_9}\right)} \quad (10)$$

$$K_{NADP} = K_d\left(\frac{k_6}{k_5+k_6}\right) = \left(\frac{k_4}{k_3}\right)\left(\frac{k_6}{k_5+k_6}\right) \quad (11)$$

$$^{D}V = ^{D}\left(\frac{V}{K_{NADP}}\right) = \frac{^{D}k_7+(^{D}K_{eq})\left(\frac{k_8}{k_9}\right)}{1+\frac{k_8}{k_9}} \quad (12)$$

where $k_6/(k_5 + k_6)$ corrects for the distribution of the central complexes between E:NADP:6PG and E′:NADP:6PG. Thus, K_{NADP} is the equilibrium constant for dissociation of $NADP^+$ from (E:NADP:6PG + E′:NADP:6PG).

On the basis of the results, the behavior of the mutant enzymes can be divided into three categories, those that exhibit an effect on binding alone, those that exhibit an effect on a step(s) other than hydride transfer, and the M13Q mutation, which exhibits a change in the rate of the hydride transfer step. Each of these categories will be discussed below.

The M13I, V Mutant Enzymes. As shown in Table 3, K_{NADP} increases by about an order of magnitude for the M13I and M13V mutant enzymes, while the $K_{i(NADPH)}$ does not change compared to that measured for the wild-type enzyme. In addition, V/E_t is unchanged, as are the isotope effects on V and V/K (the effects appear higher with the M13I enzyme, but the large error makes them within error identical); the decrease in V/K reflects the decreased affinity for NADP. Thus, although the affinity for $NADP^+$ ($\Delta\Delta G°$ 1.34 kcal/mol for both enzymes) is decreased for both mutant enzymes, once the cofactor is bound, the rate of oxidative decarboxylation is unaffected, that is, there is likely no change in the position or orientation of the 4 position of the nicotinamide ring with respect to C3 of 6PG. The main interaction of M13 is via its backbone NH with the carboxamide side chain of $NADP^+$ (*5*). Substitution of the M13 side chain with I or V should still allow the hydrogen bond to the backbone NH of the new amino acids, but their smaller side chain would not provide as large a van der Waals surface for interaction with the nicotinamide ring.

The M13F, C Mutant Enzymes. The M13F and M13C mutant enzymes also show a decrease in affinity for $NADP^+$ (9.5- and 3-fold, respectively), but no change in $K_{i(NADPH)}$. However, there is also a decrease in V/E_t of 19- and 8-fold, respectively, and an observed decrease in the isotope effect from 1.8 to 1.3 (this is a decrease of almost 3-fold in the isotope effect minus 1). Thus, in addition to the decreased affinity for cofactors, a change in the amount of rate limitation of the steps within the catalytic pathway is observed. The decreased value of V and the isotope effects suggest either a decrease in k_7 and $^{D}k_7$ or a change in the relative rates of the hydride transfer and decarboxylation steps with the former becoming faster than the latter. (An increase in the k_8/k_9 ratio will give the observed decrease in V and the isotope effects.) Since the overall rate decreases, it is likely the relative rates of hydride transfer and decarboxylation that have changed, as a result of a decrease in the rate of the decarboxylation step. The polarizable sulfur of the cysteine side chain and the potential of the aromatic ring of phenylalanine to stack with the nicotinamide ring of $NADP^+$ and NADPH may account for this phenomenon.

The M13Q Mutant Enzyme. Substitution of the glutamine side chain gives a different effect, almost certainly related to the ability of the side chain to donate and accept hydrogen bonds. Again, a decrease in the affinity for $NADP^+$ (1.34 kcal/mol) results from the mutation, and an 8-fold decrease in the overall maximum rate is observed. However, the deuterium isotope effect increases, suggesting a decrease in the rate of hydride transfer relative to decarboxylation. These effects are difficult to explain without considering a decrease in the rate of the hydride transfer step, and a change in the magnitude of the intrinsic deuterium isotope effect. Given the location of the substitution, and the nature of the potential new interactions with the side chain amide of glutamine, it is not difficult to rationalize a significant change in orientation of the nicotinamide ring of $NADP^+$ and C3 of 6PG.

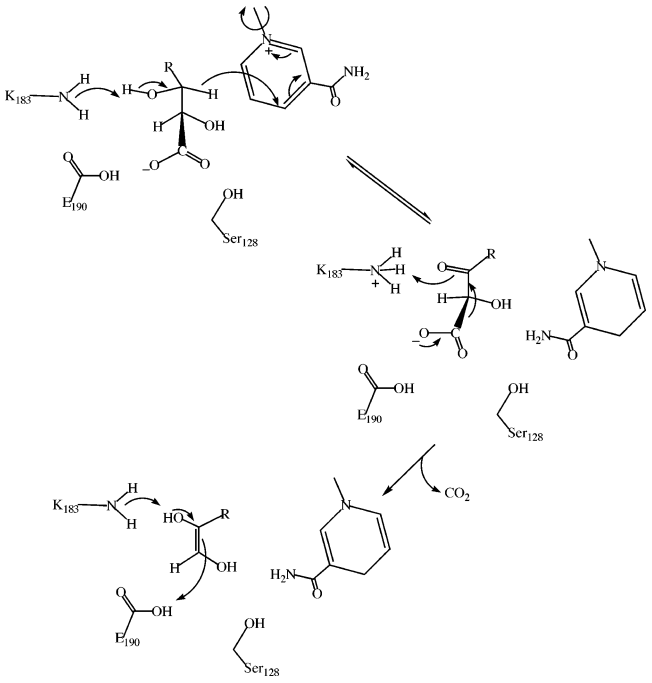

FIGURE 3: Proposed mechanism for 6-phosphogluconate dehydrogenase including the rotation of the nicotinamide ring in the oxidation step.

Proof will have to await measurement of the multiple isotope effects and/or a structure of some the mutant enzymes with $NADP^+$ bound. Nonetheless, it appears, dependent on the mutation at M13, differential effects are observed on the binding of $NADP^+$, the hydride transfer, and decarboxylation steps.

Comparison of $NADP^+$ and NADPH Affinity: Mechanistic Implications. K_{NADP} can be employed as a probe of the E:NADP:6PG dissociation constant. For all of the mutant enzymes, the affinity for $NADP^+$ decreases by about an order of magnitude, with the exception of the M13C mutation, which shows a 3-fold decreased affinity. On the other hand, the affinity of free enzyme or the E:6PG complex for NADPH does not change compared to the wild-type enzyme (with the possible exception of free enzyme in the case of the M13C mutant enzyme). Data are consistent with the structural data of Adams (*5*), which show that the side chain of M13 stacks against the nicotinamide ring of $NADP^+$ with the carboxamide oxygen within hydrogen bonding distance to the backbone NH of M13. The driving force for the rotation is likely in part due to an elimination of the electrostatic interaction between N1 of the nicotinamide ring in the oxidized cofactor, which is 5.2 Å away from the pyrophosphate backbone of the dinucleotide. In the reduced cofactor complex the distance is increased by more than 2 Å. In the case of the reduced cofactor, the nicotinamide has rotated by about 180° about the N-glycosidic bond such that the carboxamide side chain is within hydrogen bonding distance to the side chains of N187, H186, and S128, Figure 2. Of interest, the 1-carboxylate of 6PG is within hydrogen bonding distance to S128 in the E:6PG complex, while N187 is also within hydrogen bonding distance to the C3 hydroxyl of 6PG. Overall, data are consistent with the rotation of the nicotinamide ring during the course of the reaction, Figure 3. Further, since hydride transfer is from C3 of 6PG to the *si* face of the nicotinamide ring, the reaction is reversible, and the *re* face of the reduced cofactor is exposed, there is likely an equilibrium between two bound conformations of the nicotinamide, one positioned as in $NADP^+$, and another positioned like NADPH, Figure 2. The ring flip is likely required to facilitate decarboxylation, Figure 3, since the newly positioned nicotinamide of the reduced cofactor would cause a movement of the carboxylate of 3-deoxy-6PG, eliminating its interactions with E190, the general acid.

This conclusion is in accord with the mechanism proposed by Zhang et al. (*7*). In addition, data support the proposal by Rippa (*13*, *14*) for a catalytic, but nonredox role for NADPH. In this regard, it was shown that the reduced coenzyme is required in the last step of the reaction, that is, the tautomerization to the enediol of Ru5P, and NADPH can be effectively substituted with the nonreducing analogue 1,6-NADPH in this capacity (*11*, *12*). An additional nonredox role for NADPH has been demonstrated on the decarboxylation of the 3-keto intermediate of the substrate analogue 2-deoxy-6PG (*13*).

A situation analogous to the crystal structures of the E:NADP and E:NADPH complexes of 6PGDH is seen with the aldehyde dehydrogenase (*8*, *9*).The binding sites of the nicotinamide ring of NAD^+ and NADH differ. The authors suggest that the difference in conformation of the oxidized and reduced cofactors may be important to catalysis. The initial oxidation of the thiohemiacetal between the active site thiol and the substrate aldehyde by NAD^+ to give the acylenzyme intermediate requires the position of the nicotinamide near the proton to be transferred as a hydride. The authors further proposed that deacylation of the resulting thioester could be facilitated by the difference in position of the nicotinamide ring of NADH. The mechanism thus includes a rotation about the N-glycosidic bond after reduction.

Recent evidence obtained for the NAD-malic enzyme from *Ascaris suum*, an enzyme in the same class as the 6PGDH, is also suggestive of different conformers of the bound oxidized and reduced coenzyme (*47*, *48*). The position of the nicotinamide ring of NADH is rotated by >180°, compared to the NAD^+, toward the binding site of malate. Although the residue that interacts with the carboxamide side chain of NAD^+ is an asparagine, not a glycine, the situation is similar to that observed for 6PGDH with a short distance (5.7 Å) between the pyridinium N and the pyrophosphate of the coenzyme. The mechanisms proposed for the aldehyde dehydrogenase and malic enzyme are similar to that we propose for the 6PGDH. The mechanism may be common for the pyridine nucleotide-linked oxidative decarboxylases.

There are several structural features in common between 6PGDH and aldehyde dehydrogenase. (1) In both enzymes there is an absence of positively charged amino acid side chains in the vicinity of the pyrophosphate portion of the cofactor such that an ionic interaction is possible between the positive charge of the nicotinamide ring and the pyrophosphate. (2) In both enzymes rotation about the ribose to nicotinamide bond is allowed.

ACKNOWLEDGMENT

We thank Babak Andi for preparing the figures depicting the interactions of the nicotinamide ring.

REFERENCES

1. Rendina, A. R., Hermes, J. D., and Cleland, W. W. (1984) Use of Multiple Isotope Effects to Study the Mechanism of 6-Phosphogluconate Dehydrogenase, *Biochemistry 23*, 6257−6262.
2. Hwang, C. C, Berdis, A. J., Karsten, W. E., Cleland, W. W., and Cook, P. F. (1998) Oxidative Decarboxylation of 6-Phosphogluconate by 6-Phosphogluconate Dehydrogenase Proceeds by a Stepwise Mechanism with NADP and ADADP as Oxidants, *Biochemistry 37*, 12596−12602.
3. Berdis, A. J., and Cook, P. F. (1993) Overall Kinetic Mechanism of 6-Phosphogluconate Dehydrogenase from *Candida utilis*, *Biochemistry 32*, 2036−2040.
4. Price, N. E., and Cook, P. F. (1996) Kinetics and Chemical Mechanisms of the Sheep Liver 6-Phosphogluconate Dehydrogenase, *Arch. Biochem. Biophys. 336*, 215−223.
5. Adams, J. M., Grant, H. E., Gover, S., Naylor, C. E., and Phillips, C. (1994) Crystallization Studies of Coenzyme, Coenzyme Analogues, and Substrate Binding in 6-Phosphogluconate Dehydrogenase: Implications for NADP Specificity and the Enzyme Mechanism, *Structure 2*, 651−668.
6. Karsten, W. E., Chooback, L., and Cook, P. F. (1998) Glutamate 190 Is a General Acid Catalyst in the 6-Phosphogluconate Dehydrogenase-Catalyzed Reaction, *Biochemistry 37*, 15691−15697.
7. Zhang, L., Chooback, L., and Cook, P. F. (1999) Lysine 183 Is the General Base in the 6-Phosphogluconate Dehydrogenase-Catalyzed Reraction, *Biochemistry 38*, 11231−11238.
8. Hammen, P. K., Alliali-Hassani, A., Hallenga, K., Hurley, T. D., and Weiner, H. (2002) Multiple Conformations of NAD and NADH When Bound to Cytosolic and Mitochondrial Aldehyde Dehydrogenase, *Biochemistry 41*, 7156−7168.
9. Perez-Miller, S. J., and Hurley, T. D. (2003) Coenzyme Isomerization Is Integral to Catalysis in Aldehyde Dehydrogenase, *Biochemistry 42*, 7100−7109.
10. Rippa, M., Signorini, M., and Dallocchio, F. (1973) A Multiple Role for the Coenzyme in the Mechanism of Action of 6-Phosphogluconate Dehydrogenase. The Oxidative decarboxylation of 2-Deoxy-6-Phosphogluconate, *J. Biol. Chem. 248*, 4920−4925.
11. Rippa, M., Signorini, M., and Dallocchio, F. (1972) Differentiation Between the Structural and Redox Roles of TPNH in 6-Phosphogluconate Dehydrogenase, *Biochem. Biophys. Res. Commun. 48*, 764−768.
12. Rippa, M., Signorini, M., and Dallocchio F. (1973) A Role for the Pyridine of Triphosphopyridine Nucleotide in 6-Phosphogluconate Dehydrogenase, *FEBS Lett. 36*, 148−150.
13. Hanau, S., Dallocchio, F., and Rippa, M. (1992) NADPH Activates a Decarboxylation Reaction Catalyzed by Lamb Liver 6-Phosphogluconate Dehydrogenase, *Biochim. Biophys. Acta 1122*, 273−277.
14. Rippa, M., Hanau, S., Cervellati, C., and Dallocchio, F. (2000) 6-Phosphogluconate Dehydrogenase: Structural Symmetry and Functional Asymmetry, *Protein Pept. Lett. 7*, 341−348.
15. Chooback, L., Price, N. E., Karsten, W. E., Nelson, J., Sundstrom P., and Cook, P. F. (1998) Cloning, Expression, Purification, and Characterization of the 6-Phosphogluconate Dehydrogenase from Sheep Liver, *Protein Expression Purif. 13*, 251−258.
16. Silverberg, M., and Daziel, K. (1975) 6-Phospho-D-gluconate Dehydrogenase from Sheep Liver, *Arch. Biochem. Biophys. 227*, 646−651.
17. Cleland, W. W. (1977) Statistical Analysis of Enzyme Kinetic Data, *Methods Enzymol. 63*, 103−108.
18. Hwang, C. C., and Cook, P. F. (1998) Multiple Isotope Effects as a Probe of Proton and Hydride Transfer in the 6-Phosphogluconate Dehydrogenase Reaction, *Biochemistry 37*, 15698−15702.
19. Zhang, L., and Cook, P. F. (2000) Chemical Mechanism of 6-Phosphogluconate Dehydrogenase via Kinetic Studies and Site-directed Mutagenesis, *Protein Pept. Lett. 7*, 313−322.
20. Cook, P. F., Blanchard, J. S., and Cleland, W. W. (1980) Primary and Secondary Deuterium Isotope Effects on the Equilibrium Constant for Enzyme Catalyzed Reactions, *Biochemistry 19*, 4853−4858.
21. Tsui, S. K., Chan, J. Y., Waye, M. M., Fung, K. P., and Lee, C. Y. (1996) Identification of a cDNA Encoding 6-Phosphogluconate Dehydrogenase from a Human Heart cDNA Library, *Biochem. Genet. 34*, 367−373.
22. Somers, D., Medd, S. M., Walkert, J. E., and Adams, M. J. (1992) Sheep 6-Phosphogluconate Dehydrogenase. Revised Protein Sequence Based Upon the Sequences of a cDNA Clone Obtained with the Polymerase Chain Reaction, *Biochem. J. 288*, 1061−1067.
23. Fahrendorf, T., Ni, W., Shorrosh, B. S., and Dixon, R. A. (1995) Stress Responses in Alfalfa (*Meticago sativa* L.) XIX. Transcriptional Activation of Oxidative Pentose Genes at the Onset of the Isoflavinoid Phytoalexin Responses, *Plant Mol. Biol. 28*, 885−900.
24. Wang, R. F., Khan, A. A., Cao, W. W., and Cerniglia, C. E. (1998) Identification and Sequencing of a cDNA Encoding 6-Phosphogluconate Dehydrogenase from a Fungus, *Cuninghamella elegans*, and Expression of the Gene in *Escherichia coli*, *FEMS Microbiol. Lett. 169*, 397−402.
25. Gloekner, F. O., Kube, M., Bauer, M., Teeling, H., Lombardot, T., Ludwig, W., Gade, D., Beck, A., Borzym, K., Heitmann, K., Rabus, R., Schlessner, H., Amann, R., and Reinhardt, R. (2003) Complete Genome Sequence of the Marine Planctomycete *Pirellula* sp. Strain 1, *Proc. Natl. Acad. Sci. U.S.A. 100*, 8298−8303.
26. Scott, M. J., and Lucchesi, J. C. (1991) Structure and expression of the *Drosophila melanogaster* Gene Encoding 6-Phosphogluconate Dehydrogenase, *Gene 109*, 177−183.
27. Tsui, S. K., Chan, J. Y., Waye, M. M., Fung, K. P., and Lee, C. Y. (1996) Identification of a cDNA Encoding 6-Phosphogluconate Dehydrogenase from a Human Heart cDNA Library, *Biochem. Genet. 34*, 367−373.
28. Barret, M. P., and Le Page, R. W. F. (1993) A 6-Phosphogluconate Dehydrogenase Gene from *Trypanosoma brucei*, *Mol. Biochem. Parasitol. 57*, 89−100.
29. Bao, Q., Tian, Y., Li, W., Xu, Z., Xuan, Z., Hu, S., Dong, W., Yang, J., Chen, Y., Xue, Y., Xu, Y., Lai, X., Huang, L., Dong, X., Ma, Y., Ling, L., Tan, H., Chen, R., Wang, J., Yu, J., and Yang, H. (2002) A Complete Sequence of the *T. tengcongensis* Genome, *Genome Res. 12*, 689−700.
30. Mazzoni, C., Ruzzi, M., Rinaldi, T., Solinas, F., and Montebova, F., Frontali, L. (1997) Sequence Analysis of a 10.5 kb DNA Fragment from the Yeast Chromosome VII Reveals the Presence of Three New Open Reading Frames and a tRNA Thr gene, *Yeast 13*, 369−372.
31. Tamas, I., Klasson, L., Canbach, B., Naslund, A. K., Eriksson, A. S., Wernergreen, J. J., Sandstrom, J. P., Moran, N. A., and Andersson, S. C. (2002) 50 Million Years of Genomic Stasis in Endosymbiotic Bacteria, *Science 296*, 2376−2379.
32. Nasoff, M. S., Baker, H. V., II, and Wolff, R. E., Jr. (1984) DNA Sequence of the *Escherichia coli* Gene, *gnd*, for 6-Phosphogluconate Dehydrogenase, *Gene 27*, 253−257.
33. Morona, R., Mavris, M., Fallarino, A., and Manning, P. A. (1994) Characterization of the *rfc* Region of *Shigella flexneri*, *J. Bacteriol. 176*, 733−747.
34. Reeves, P., and Stevenson, G. (1989) Cloning and Nucleotide Sequence of the *Salmonella typhimurium* LT2 *gnd* Gene and its Homology with the Corresponding Sequence of Escherichia coli K12, *Mol. Gen. Genet. 217*, 182−184.
35. Akarawa, Y., Wacharotayankun, R., Nagatsuka, T., Ito, H., Kato, N., and, Otha, M. (1995) Genomic Organization of the *Klebsiella pneumoniae* cps Region Responsible for Serotype K2 Capsular Polysaccharide Synthesis in the Virulent Strain Chedid, *J. Bacteriol. 177*, 1788−1796.
36. Tetaud, E., Hanau, S., Wells, J. M., Le Page, R. W. F., Adams, M. J., Arkinson, S., and Barret, M. P. (1999) 6-Phosphogluconate Dehydrogenase from *Lactococcus lactis*: A Role for Arginine Residues in Binding Substrates and Coenzyme, *Biochem. J. 338*, 55−60.
37. Yoshida, Y., Nakano, Y., Yamashita, Y., and Koga, T. (1997) The *gnd* Gene Encoding a Norl 6-Phosphogluconate Dehydrogenase and its Adjacent Region of *Actinobacillus actinomycetemcomitans* Chromosal DNA, *Biochem. Biophys. Res. Commun. 230*, 220−225.
38. Kaneko, T., Tanaka, A., Sato, S., Totani, H., Suzuka, T., Miyajima, N., Sugiura, M., and Tabata, S. (1995) Sequence Analysis of the Genome of the Unicellular *Synechocystis* sp Strain PCC6803. I. Sequence Features in the 1 Mb Region from Map Position 64% to 92% of the Genome, *DNA Res. 2*, 153−166.
39. Broedel, S. E., Jr., and Wolf, R. E., Jr. (1990) Growth-Phase-Dependent Induction of 6-Phosphogluconate Dehydrogenase and Glucose 6-phosphate Dehydrogenase in the Cyanobacterium *Synechococcus* sp. PCC7942, *J. Bacteriol. 172*, 4023−4031.
40. Fleischmann, R. D., Adams, M. D., White, O., Clayton, R. A., Kirkness, E. F., Kerlavage, A. R., Bult, C. J., Tomb, J. F.,

Dougherty, B. A., Merrick, J. M., Mckenney, K., Sutton, G., Fithugh, W., Fields, C. A., Gocaine, J. D., Scott, J. D., Shirley, R., Liu, L.-I, Glodek, A., Kelley, J. M., Weidman, J. F., Phillips, C. A., Spriggs, T., Hedblom, E., Cotton, M. D., Utterback, T. R., Hanna, M. C., Nguyen, D. T., Saudek, A. D. M., Brandon, R. C., Fine, L. D., Frichman, J. L., Fuhrmann, J. L., Geoghagen, N. S. M., Gnehm, C. L., Mcdonald, L. A., Small, K. V., Fraser, C. M., Smith, H. O., and Venter, J. C. (1995) Whole Genome Random Sequence and Assembly of *Haemophilus influenzae* RD, *Science 269*, 496−512.

41. Scott, M. J., Kricticou, D., and Robinson, A. S. (1993) Isolation of cDNAs Encoding 6-Phosphogluconate Dehydrogenase and Glucose 6-phosphate Dehydrogenase from the Mediterranean Fruit Fly *Ceratitis capitata*: Correlating Genetic and Physiologic Maps of Chromosome 5, *Insect. Mol. Biol. 1*, 213−222.
42. Fraser, C. M., Norris, S. J., Weinstock, G. M., White, O., Sutton, G. G., Dodson, R. J., Gwinn, M. L., Hickey, E. K., Clayton, R. A., Ketchum, K. A., Sodegren, E., Hardham, J. M., Mcleod, M. P., Salzberg, S. L., Peterson, J. D., Khalak, H. G., Richardson, D. L., Howell, J. K., Chidambaram, M., Utterback, T. R., McDonald, L. A., Artiach, P., Bowman, C., Cotton, M. D., Fujii, C., Garland, S. A., Hatch, B., Horst, K., Roberts, K. M., Sandusky, M., Weidman, J. F., Smith, H. O., and Venter, J. C. (1998) Complete Genome Sequence of *Treponema pallidum*, the Syphilis Spirochete, *Science 281*, 375−388.
43. Yoshida, K., Seki, S., and Fujita, Y. (1994) Nucleotide Sequences and Features of the *Bacillus lichenformis gnt* Operon, *DNA Res. 1*, 157−162.
44. Fujita, Y., Fujita, T., Miwa, Y., Nihashi, J., and Aratani, Y. (1986) Organization and Transcription of the Gluconate Operon, *gnt*, of *Bacillus subtilis*, *J. Biol. Chem. 261*, 13744−13753.
45. Eiglmeier, K., Honore, N., Woods, S. A., Caudron, B., and Cole, S. T. (1993) Use of an Ordered Cosmid Library to Deduce the Genomic Organization of *Mycobacterium leprae*, *Mol. Microbiol. 7*, 197−206.
46. Stephens, R. S., Kalman, S., Lammel, C. J., Fan, J., Marathe, R., Aravind, L., Mitchell, W. P., Olinger, L., Tatusoy, R. L., Zhao, Q., Koonin, E. V., and Davis, R. W. (1998) Genome Sequence of an Obligate Intracellular Pathogen of Humans: *Chlamydia trachomatis*, *Science 282*, 754−759.
47. Coleman, D. E., Rao, G. S. J., Goldsmith, E. J., Cook, P. F., and Harris, B. G. (2002) Crystal Structure of the Malic Enzyme from *Ascaris suum* Complexed with Nicotinamide Adenine Dinucleotide at 2.3 Å Resolution, *Biochemistry 41*, 6928−6938.
48. Rao, G. S. J., Coleman, D. E., Karsten, W. E., Cook, P. F., and Harris, B. G. (2003) Crystallographic Studies on *Ascaris suum* NAD-Malic Enzyme Bound to Reduced Cofactor and Identification of an effector Site, *J. Biol. Chem. 278*, 38051−38058.

BI0476679